# PIANO HAMMER-STRING CONTACT DURATION: HOW THE BASS HAMMER IS RELEASED FROM THE STRING

*Anatoli Stulov*

Institute of Cybernetics at Tallinn University Technology, Estonia
stulov@ioc.ee

**ABSTRACT**

We associate the bass hammer-string contact duration with the time of propagation of compression wave traveling through the hammer body from the contact point to the hammer kernel and back. Based on the hereditary model of the microstructured wool felt, it has been revealed that the stiffness of felt is a nonlinear function of the compression and it is strongly determined by the rate of the felt loading. This means that the speed of the compression wave that propagates through the felt depends on the wave form and on its amplitude. It has been shown that the pulse of a smooth form, and which has no discontinuity on its front propagates with constant speed until the accumulation of nonlinear effects results in the eventual continuous wave breaking. After that moment the shock has been formed, and now the velocity of the shock wave depends on the value of the jump discontinuity across the wave front. It has been shown that the front velocity of the shock wave is greater than the velocity in a linear medium. Therefore, the total time of wave propagation, which is related with a duration of the hammer-string contact, decreases as the dynamic level of the hammer impact is raised. As result, for the first bass hammers the contact duration is shorter than the round-trip time to agraffe, and hence, no reflected wave is needed to assist the hammer for going away from the string.

## 1. INTRODUCTION

The process of the string excitation by a hammer impact is under investigation for a plenty of years. There are many studies devoted to this problem. We may recollect the well known reviews by Hall [1], Suzuki and Nakamura [2], and Fletcher and Rossing [3].

By now, it is well known that the duration of the hammer-string contact time is one of the main parameters in determining the spectral content of the sound produced by a piano. The problem of the contact duration between the hammer and the string, and discussion what can cause the hammer to rebound is a central point of many papers. The prevailing view about this question is presented in [4, 5, 6].

The common understanding of the dynamics of the hammer-string interaction is expressed in [5]: *"When the hammer has less mass than the string, it will most likely be thrown clear of the string by the first reflected pulse."*

Nevertheless, the assumptions that only the first reflected wave can rebound the hammer from the string is not quite true. For example, in [7] it was found that the contact duration for *A1* note is less than the round-trip time to agraffe. In addition, in [1], and in [6] it is definitely stated that the hammer can rebound from the string without the assistance of any reflected wave.

This problem was also considered in [8], and by using the nonlinear hysteretic hammer felt model it was shown that the bass hammers, which are relatively light compared to the string, may lose string contact due to the hammer elasticity, and without the assistance of waves traveling along the string, and reflecting back from the agraffe.

This fact is illustrated by Fig. 1.

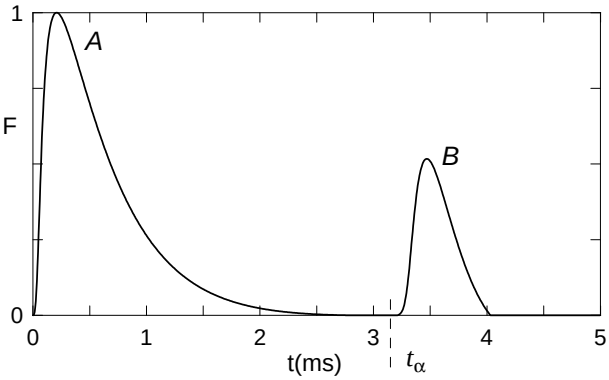


Figure 1: Normalized force history of the hammer-string interaction. Hammer number $N$ = 6 (note $D_1$: $f$ = 36.71 Hz); initial hammer impact velocity is 5 m/s. $t_\alpha$ is the moment of reflected wave arrival.

The numerical simulation of the hammer-string interaction shows that the acting force exerted by the hammer impact consists of two pulses. The first pulse $A$ displays the process of loading and unloading of the hammer during the impact. The moment of arrival of the first reflected wave from the agraffe is marked by $t_\alpha$. It means that the hammer has time enough to decompress fully, and moves away from the string without the assistance of reflected wave.

After the moment $t_\alpha$ the reflected wave arrives to the contact point, and one can see the beginning of the second, or repeated contact between the hammer and the string (pulse $B$). This process is presented in Fig. 1 definitely.

The goal of the current paper is to understand the physics of the hammer unloading through the traveling waves, but traveling not along the string, but by means of compression waves propagated inside the hammer body, which stiffness is essentially nonlinear.

## 2. COMPRESSION WAVES IN THE FELT

We associate the contact duration with a time, which is needed for a wave traveling with velocity $c$ to spread for a distance $L = 2\lambda$, where $\lambda$ is the felt thickness. The simple scheme of wave propagation through the hammer body is shown in Fig. 2.

In order to analyze the process of compression wave propagation in the hammer felt, and to estimate the speed of that wave, the constitutive equation of the microstructured wool felt

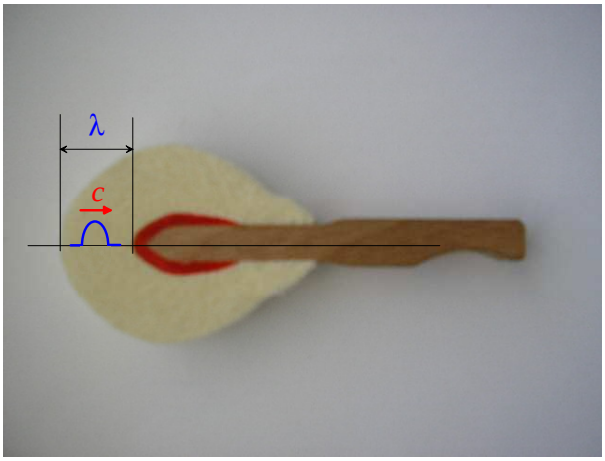


Figure 2: Hammer wave parameters.

material was derived in [9] in the form

$$\sigma(\varepsilon) = E_d \left[ \varepsilon^p(t) - \frac{\gamma}{\tau_0} \int_{-\infty}^{t} \varepsilon^p(\xi) \exp\left(\frac{\xi - t}{\tau_0}\right) d\xi \right]. \quad (1)$$

Here $\sigma$ is the stress, $\varepsilon = \partial u/\partial x$ is the strain, $u$ is the displacement, the constant $E_d$ is the dynamic Young's modulus of the felt, $p$ is the parameter of nonlinearity, $\gamma$ is the hereditary amplitude, and $\tau_0$ is the relaxation time.

Because this approach is based on the piano hammer model [10, 11], we are limited to describing only the compression wave propagation ($\varepsilon(x,t) > 0$).

The one-dimensional strain wave propagation in the wool felt is considered in [9]. By using the classical equation of motion

$$\rho \frac{\partial^2 u}{\partial t^2} = \frac{\partial \sigma}{\partial x}, \quad (2)$$

where $\rho$ is the felt density, and the constitutive equation (1), a nonlinear partial differential equation with third-order terms is derived in the following form

$$\rho \frac{\partial^2 u}{\partial t^2} + \rho\tau_0 \frac{\partial^3 u}{\partial t^3} - E_d \left\{ (1-\gamma) \frac{\partial}{\partial x} \left[ \left( \frac{\partial u}{\partial x} \right)^p \right] + \tau_0 \frac{\partial^2}{\partial x \partial t} \left[ \left( \frac{\partial u}{\partial x} \right)^p \right] \right\} = 0. \quad (3)$$

The dimensionless form of this equation is obtained by using the non-dimensional variables that are introduced by the relations

$$u \Rightarrow u/l_0, \quad x \Rightarrow x/l_0, \quad t \Rightarrow t/\alpha_0, \quad (4)$$

where

$$\alpha_0 = \tau_0/\delta, \quad l_0 = \tau_0 \sqrt{E_d/\delta\rho}, \quad (5)$$

and parameter $\delta$ is defined as $0 < \delta = 1 - \gamma \leqslant 1$.

In terms of non-dimensional strain variable $\varepsilon(x,t)$ Eq. (3) reads

$$(\varepsilon^p)_{xx} - \varepsilon_{tt} + (\varepsilon^p)_{xxt} - \delta\varepsilon_{ttt} = 0. \quad (6)$$

Several samples of felt pads were subjected to the static stress-strain tests in mechanical laboratory at the Faculty of Civil Engineering at the Tallinn University of Technology. The average value of the static Youngs modulus of the pads was estimated as $E_s = 0.06$ MPa. The value of the felt density was determined as $\rho \approx 10^3$ kg/m$^3$.

For numerical simulation the reasonable value of the static Young's modulus of the felt is chosen to be $E_s = 0.05$ MPa. The values of hereditary parameters are chosen as $\gamma = 0.99$ and $\tau_0 = 14$ $\mu$s, which are close to the values of the same parameters for bass piano hammers [12].

Taking into account the relationship $E_s = \delta E_d$ that is derived in [9], we obtain

$$\delta = 0.01, \quad E_d = 5 \text{ MPa}, \quad c_s = 7 \text{ m/s}, \quad c_d = 70 \text{ m/s}. \quad (7)$$

Here velocity $c_s = \sqrt{E_s/\rho}$ corresponds to the static Young's modulus $E_s$ (very slow loading), and velocity $c_d = \sqrt{E_d/\rho}$ corresponds to the dynamic Young's modulus $E_d$ (very fast loading).

By using these values of material constants, the space scale $l_0$ and time scale $\alpha_0$ that were used in (4) are

$$l_0 = 10 \text{ mm}, \quad \alpha_0 = 1.4 \text{ ms}. \quad (8)$$

The numerical analysis of the strain wave propagation is presented in [9]. This calls for solution of the boundary value problem of Eq. (6). A boundary value of the strain prescribed at $x = 0$ is selected in the following form

$$\varepsilon(0,t) = A \left( \frac{t}{t_m} \right)^3 e^{3(1 - t/t_m)}, \quad (9)$$

where $t_m$ defines the time coordinate corresponding to the maximum of the pulse amplitude $A$.

This form of a pulse is continuous and smooth, and it is very similar to the force history pulse shown in Fig. 4a in [12]. The front of a pulse satisfies necessary conditions $\varepsilon(0,0) = \varepsilon_t(0,0) = \varepsilon_{tt}(0,0) = 0$.

The effect of the value of initial pulse amplitude $A$ on the pulse evolution is presented in Fig. 3. The material parameters are selected as $\delta = 0.2$ and $p = 1.5$. The numerical solution is presented for three sequential time moments, and for three different values of the initial amplitude $A$ of the boundary value (9).

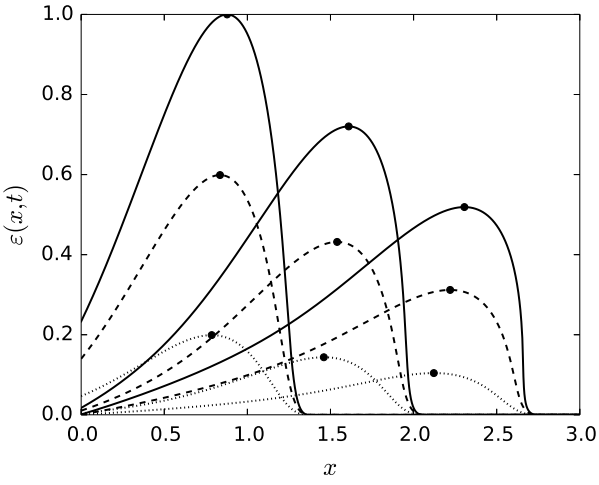


Figure 3: Nonlinear evolution of a pulse ($t_m = 1/2$) for time moments $t = 2$, $t = 3$ and $t = 4$. Pulses of an initial amplitude $A = 0.1$ are shown by solid lines, $A = 0.06$ by dashed lines, $A = 0.02$ by dotted lines. Bullets show the position of the pulse maximum. The results have been normalized relative to the largest amplitude ($A = 0.1$).

One can see, that in this case the front velocity is a constant value $V_f = c_s$, and does not depend on the pulse amplitude. On the other hand, it is also evident that for larger amplitudes

the maximum point, or the crest of a pulse (shown by bullets), propagates faster than the front of a pulse.

Therefore a forward-facing slope of a pulse becomes steeper with a distance of propagation, and accumulation of this effect results in the finally pulse breaking. This means that the shock wave will be formed at the moment when the forward-facing slope of a pulse becomes vertical, and therefore the value of discontinuity across the wave front is defined by the amplitude of a pulse crest.

## 3. SHOCK WAVE PROPAGATION

Here we consider propagation of a pulse with a finite jump discontinuity on the front through the felt material. For any rate of loading the felt material is defined with the aid of the nonlinear constitutive equation (1) in the form

$$\sigma(U) = E_d \left[ (U_x)^p - \frac{\gamma}{\tau_0} \int_{-\infty}^{t} (U_x)^p \, e^{(\omega - t)/\tau_0} d\omega \right]. \quad (10)$$

Here the values of parameters are: $p > 1$, and $0 \leqslant \gamma < 1$.

The conservation law

$$\frac{d}{dt} \int_{x_1}^{x_2} \rho U_{tt}(x,t) dx = \sigma(x_2,t) - \sigma(x_1,t) \quad (11)$$

gives a correspondence between the shock conditions and the shock velocity $V_s$

$$[\sigma] = -\rho V_s [U_t], \quad (12)$$

where the brackets indicate the jump in the quantity [13].

The constitutive equation in the form (10) gives a relationship

$$[\sigma] = E_d [U_x]^p. \quad (13)$$

By using (12), (13), and taking into account the kinematic identity $[U_t] = -V_s[U_x]$, one can find the relationship between the anticipated front velocity $V_s$ and the value of the discontinuity $[U_x]$ across the wave front

$$\upsilon = \frac{V_s}{c_d} = [U_x]^{\frac{p-1}{2}}, \quad [U_x] = [\varepsilon] = \varepsilon_0 = \text{const} > 0. \quad (14)$$

The dependence of non-dimensional front velocity on the value of discontinuity across the wave front is shown in Fig. 4a.

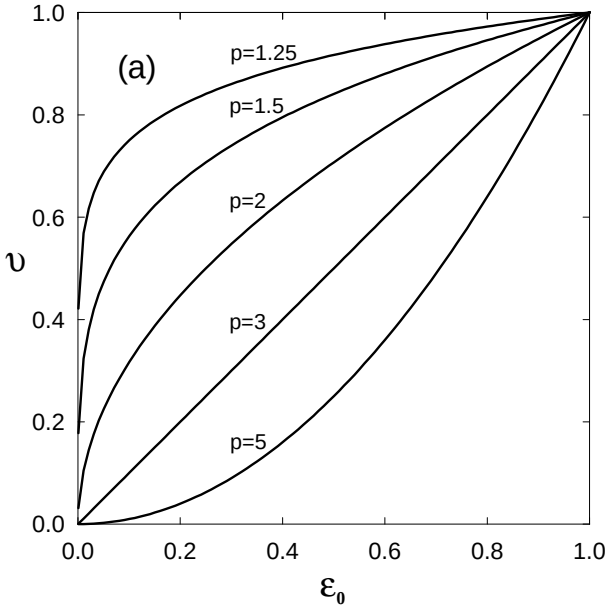


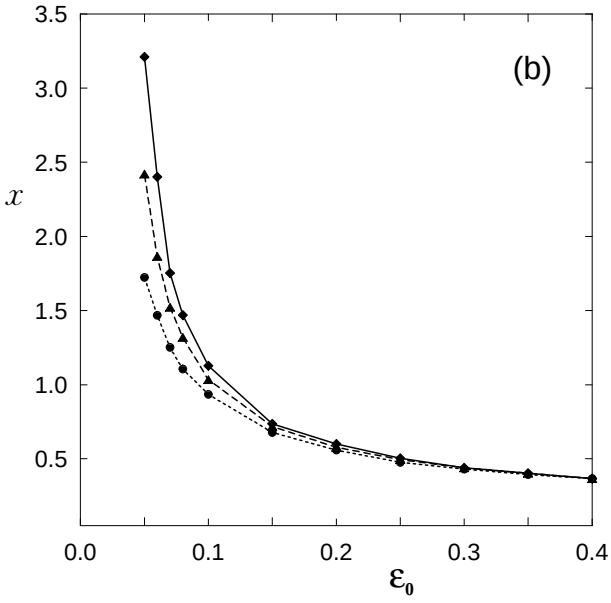


Figure 4: Shock wave parameters as functions of the value of discontinuity $\varepsilon_0$ across the wave front. (a) Non-dimensional front velocity $\upsilon$ shown for various values of parameter $p$. (b) Non-dimensional distance $x$ of the shock formation shown for various values of parameter $\delta$ = 0.01 (diamonds), $\delta$ = 0.2 (triangles), and $\delta$ = 0.6 (bullets).

As it was mentioned above, in the linear case, and for the continuous smooth pulse ($\varepsilon_0$ = 0), the front velocity is a constant value $V_f = c_s$. In case of the shock wave propagation ($\varepsilon_0 > 0$), the front velocity $V_s$ is always greater than $V_f$, because $c_d > c_s$ (see relationships (7)).

By numerical simulation of the strain wave propagation, whose initial form is given by the smooth and continuous boundary value (9), the distances, at which the shock pulse is formed, were specified, and the values of discontinuity across the wave front at these points were determined. These dependencies of the distance $x$ of the shock wave appearance as a function of the value of discontinuity $\varepsilon_0$ across the wave front for various values of parameter $\delta$ are presented in Fig. 4b.

## 4. CONCLUDING REMARKS

Resuming the results presented above, we can state that the strain (compression) wave, which originally is continuous and smooth enough, initially propagates through the felt material with a constant speed $V_f = c_s$, until the shock pulse is formed. After that moment the pulse propagates with a velocity $V_s > V_f$, and this shock velocity depends on the value of the discontinuity $\varepsilon_0$ across the wave front, which, in turn, depends on the initial level of the hammer impact.

Finally, using the data obtained, we can estimate the average velocity $V_{av}$ of the wave propagating through the hammer felt. We associate this velocity $V_{av}$ with compression wave velocity $c$ shown in Fig. 2.

For a numerical example we have chosen the nonlinear parameter $p$ = 1.5, and the distance of wave propagation $L = 2\lambda$ = 32 mm, which is equal approximately to the double thickness of the felt of first bass hammer. The values of other parameters, such as the space scale $l_0$ and the time scale $\alpha_0$, are the same as presented in (7) and (8). The non-dimensional parameters $x$ and $\upsilon$ are obtained by using the results presented in Fig. 4.

| $\varepsilon_0$ | $x(1)$ | $X$(mm) | $t_1$(ms) | $L_x$(mm) | $\upsilon(1)$ | $V_s$(m/s) | $t_2$(ms) | $t_*$(ms) | $V_{av}$(m/s) |
|---|---|---|---|---|---|---|---|---|---|
| 0.05 | 3.20 | 32.0 | 4.57 | 0 | 0.473 | 47.3 | 0 | 4.57 | 7.0 |
| 0.075 | 1.75 | 17.5 | 2.50 | 14.5 | 0.523 | 52.3 | 0.28 | 2.78 | 11.5 |
| 0.10 | 1.13 | 11.3 | 1.15 | 20.7 | 0.562 | 56.2 | 0.37 | 1.52 | 21.0 |
| 0.15 | 0.74 | 7.4 | 1.06 | 24.6 | 0.622 | 62.2 | 0.39 | 1.45 | 22.0 |
| 0.20 | 0.60 | 6.0 | 0.86 | 26.0 | 0.669 | 66.9 | 0.40 | 1.26 | 25.4 |

Table 1: Parameters of traveling compression wave.

The other parameters displayed in Table 1 are determined by relations

$$X = xl_0,\ \ L_x = L - X,\ \ V_s = \upsilon c_d,\ \ t_1 = X/c_s,$$

$$t_2 = L_x/V_s,\ \ t_* = t_1 + t_2, \quad V_{av} = L/t_*. \qquad (15)$$

Here $X$ is the distance that the wave propagates through a felt with a "normal" speed $c_s$ in the time $t_1$, $L_x$ is the part of a whole distance $L = 2\lambda$ (see Fig. 2) through which the wave propagates in the time $t_2$ with the velocity $V_s$, and $t_*$ is the total time of propagation. The velocity $V_{av}$ is the "average" speed of traveling wave.

Analysis of the data presented in Table 1 shows that the wave with a small initial amplitude, which results in the value of jump discontinuity across the wave front $\varepsilon_0$ = 0.05, propagates through the whole distance as a smooth pulse. This small amount of the compression amplitude one can relate with $pp$ dynamical level of a hammer blow, which corresponds to the velocity of the hammer impact $V$ = 1 m/s, approximately.

On the contrary, the value of discontinuity across the wave front $\varepsilon_0$ = 0.2 can be created only by a very hard $ff$ level of a hammer blow, which corresponds to the initial hammer velocity $V$ = 7 m/s, approximately.

The total time of the wave propagation $t_*$ one can associate with the duration of contact between the hammer and the string. After this moment $t_*$ the hammer felt is unloaded completely, and the hammer has lost the contact with the string.

Thus, with the growth of the level of the hammer impact and the shock pulse appearance, the average speed $V_{av}$ of wave propagation increases.

Therefore, we can state that the duration of the hammer-string contact decreases as the dynamic level of the hammer impact is raised, and this effect is appeared due to a peculiar property of the piano hammer felt, which is called the nonlinear hammer stiffness.

## 5. ACKNOWLEDGMENT

This research was supported by the European Regional Development Fund (Project TK124 (CENS)).

## 6. REFERENCES

[1] D. E. Hall, "Piano string excitation III: General solution for a soft narrow hammer," *J. Acoust. Soc. Am.*, vol. 81, no. 2, pp. 547–555, 1987.

[2] H. Suzuki and I. Nakamura, "Acoustics of pianos," *Appl. Acoustics*, vol. 30, pp. 147–205, 1990.

[3] N. H. Fletcher and Th. D. Rossing, *The Physics of Musical Instruments*, Springer, New York, 2nd edition, 1998.

[4] D. E. Hall, "Piano string excitation in the case of small hammer mass," *J. Acoust. Soc. Am.*, vol. 79, no. 1, pp. 141–147, 1986.

[5] Th. D. Rossing, *The Science of Sound*, Addison-Wesley, 2nd edition, 1990.

[6] A. Askenfelt and E. V. Jansson, "From touch to string vibrations. III: String motion and spectra," *J. Acoust. Soc. Am.*, vol. 93, no. 4, Pt.1, pp. 2181–2196, 1993.

[7] T. Yanagisawa and K. Nakamura, "Dynamic compression characteristics of piano hammer felt," *J. Acoust. Soc. Jpn.*, vol. 40, no. 11, pp. 725–729, 1984.

[8] A. Stulov, "Piano hammer - string interaction," in *Proceedings of ICA 2004*, Kyoto, Japan, 2004, pp. 2127–2130.

[9] D. Kartofelev and A. Stulov, "Propagation of deformation waves in wool felt," *Acta Mechanica*, vol. 225, pp. 3103–3113, 2014.

[10] A. Stulov, "Hysteretic model of the grand piano hammer felt," *J. Acoust. Soc. Am.*, vol. 97, no. 4, pp. 2577–2585, 1995.

[11] A. Stulov, "Dynamic behavior and mechanical features of wool felt," *Acta Mechanica*, vol. 169, pp. 13–21, 2004.

[12] A. Stulov, "Experimental and computational studies of piano hammers," *Acta Acoustica united with Acoustica*, vol. 91, no. 6, pp. 1086–1097, 2005.

[13] G. Whitham, *Linear and Nonlinear Waves*, Wiley-Interscience, New York, 1974.